Anomalous Hall Effect in the Dirac Semimetal Cd_3As_2 Probed by In-Plane Magnetic Field

Shinichi Nishihaya,[1] Hiroaki Ishizuka,[1] Yuki Deguchi,[1] Ayano Nakamura,[1] Tadashi Yoneda,[1] Hsiang Lee,[1] Markus Kriener,[2] and Masaki Uchida[1,3,*]

[1]*Department of Physics, Institute of Science Tokyo, Tokyo 152-8551, Japan*
[2]*RIKEN Center for Emergent Matter Science (CEMS), Wako 351-0198, Japan*
[3]*Toyota Physical and Chemical Research Institute (TPCRI), Nagakute 480-1192, Japan*

(Received 6 April 2025; revised 11 June 2025; accepted 17 July 2025; published 2 September 2025)

Intrinsic anomalous Hall effect (AHE) formulated by geometric properties of Bloch wave functions is a ubiquitous transport phenomenon not limited to magnetic systems but also allowed in nonmagnetic ones under an external field breaking time-reversal symmetry. On the other hand, detection of field-induced AHE is practically challenging because the band modulation through the Zeeman and spin-orbit couplings is typically small compared to other contributions as induced by the Lorentz force. Here, we demonstrate on Dirac semimetal Cd_3As_2 films that the field-induced AHE in nonmagnetic systems can be quantitatively probed by applying and rotating the magnetic field within the Hall deflection plane. Measurements on the Cd_3As_2 (112) plane reveal that AHE emerges as a clear threefold symmetric component for the in-plane field rotation. This intrinsic response becomes more pronounced in ultralow-electron-density films where significant variations in the geometric properties are expected under the magnetic field. Our findings open new opportunities in the research of Hall responses manifested as orbital magnetization in nonmagnetic systems.

DOI: 10.1103/5d7l-mr7k

Recently, the anomalous Hall effect (AHE) has been under intense focus as a measure of the geometric properties of the Bloch wave functions. Contrary to the early phenomenological belief that AHE is proportional to the out-of-plane spin magnetization, the modern formulation based on Berry curvature [1] has clarified that it is not limited to systems with sizable magnetization, but also allowed in antiferromagnets with a vanishingly small magnetization [2] and even in nonmagnetic systems [3–5], as long as the Berry curvature integrated over the occupied states remains finite under time-reversal symmetry broken conditions. In contrast to AHE in magnetic systems with spontaneous magnetization [Fig. 1(a)], emergence of AHE in nonmagnetic systems indicates the generation of effective out-of-plane magnetization component by external fields, which breaks the time reversal symmetry [3,6,7]. One related example is the nonlinear Hall effect reported in inversion-symmetry-broken systems, where the nonzero Berry curvature dipole combined with an electric field applied normal to it induces Hall response and out-of-plane orbital magnetization even under zero magnetic field [8,9]. On the other hand, orbital magnetization as a direct consequence of nonzero Berry curvature can also be generated by a magnetic field through Zeeman and spin-orbit couplings as shown in Fig. 1(b). In principle, the magnetic-field-induced AHE should appear in nonmagnetic systems, which, however, has rarely been reported due to its small amplitude typically overwhelmed by other contributions as induced by the Lorentz force.

As for the experimental detection of the magnetic-field-induced AHE, a sufficiently large modulation of the band structure by the magnetic field is required. In this respect, promising candidates are gapless semimetals or narrow-gapped semiconductors with a large g factor which can form topological band (anti-)crossings hosting giant Berry curvature under the magnetic field. In fact, unconventional responses attributed to the anomalous Hall or Nernst effect have been reported in pioneering studies of nonmagnetic systems such as the Dirac semimetal Cd_3As_2 [10] and the massive Dirac semimetal $ZrTe_5$ [11,12]. However, the observed field dependence implies a coexistence of different contributions, hindering the quantification of AHE. Actually, it is challenging to identify the field-induced AHE measured under the conventional out-of-plane field configuration, since the measured transverse response is dominated by Lorentz-force effects. Namely, the field-linear component of AHE is not distinguishable from the single-carrier ordinary Hall effect (OHE). Even if there is a nonlinear or nonmonotonic component of AHE, it is practically difficult to exclude possible multicarrier OHE or other inhomogeneity-induced effects, especially in low-carrier density samples.

Here, we focus on the possibility that the field-induced AHE in nonmagnetic systems can be probed by an in-plane

*Contact author: m.uchida@phys.sci.isct.ac.jp

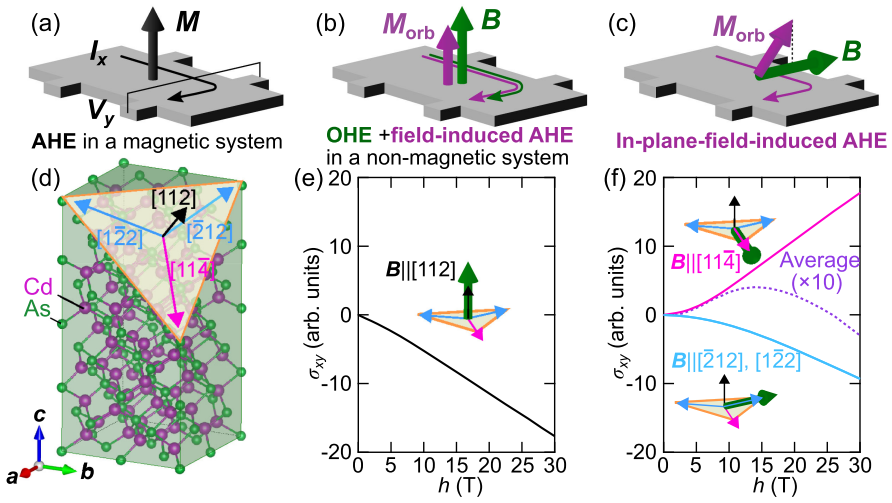

FIG. 1. Field-induced anomalous Hall effect in nonmagnetic Cd_3As_2. (a) Anomalous Hall effect (AHE) in a magnetic system with spontaneous magnetization, (b) ordinary Hall effect (OHE) and field-induced AHE in a nonmagnetic system under the out-of-plane field, and (c) AHE induced by an in-plane field applied to the crystal plane with oddfold rotational symmetry about its out-of-plane direction. (d) (112) plane of Cd_3As_2 highlighted in its tetragonal structure, which allows the observation of both onefold and threefold symmetric in-plane AHE for the in-plane field rotation. Field-induced Hall conductivities calculated for (e) the out-of-plane field $B\|[112]$ and (f) the in-plane fields $B\|[\bar{1}\,\bar{1}\,4]$, $[2\bar{1}\,\bar{2}]$, and $[\bar{1}2\bar{2}]$. The dashed line indicates the average of the contributions from the three crystal domains rotated by 120°, which corresponds to the threefold component of the in-plane AHE.

magnetic field. With fulfilling symmetry conditions [13,14], out-of-plane Berry curvature and associated orbital magnetization can be induced even by the in-plane field, leading to in-plane AHE as illustrated in Fig. 1(c). Being a field-odd effect, in-plane AHE is only allowed on the crystal plane with oddfold rotational symmetry about its out-of-plane axis [13,14]. Following many theoretical proposals [4,5,15–22], in-plane AHE with threefold rotational symmetry has been reported in various magnetic systems [23–27]. The field-induced Hall response up to the B^1 order with onefold rotational symmetry has been observed in several nonmagnetic systems [11,28,29], and it has been proposed to link to the quantum geometric quantities of the band structure as formulated by extended semiclassical theories [5,20,21]. On the other hand, the in-plane AHE proportional to B^3 on a plane with C_3 symmetry, such as the (001) plane of a trigonal system [23–25] or the (111) plane of a cubic system [27] offers exceptional advantages for quantifying the in-plane AHE. The anomalous Hall response with a threefold symmetric feature for the in-plane field rotation can be easily separated from the Lorentz-force induced OHE either due to the slight sample misalignment or due to the selection of a low-symmetry plane with nonzero off-diagonal components in the Hall conductivity tensor [30,31], all of which contribute to the onefold symmetric component.

In this Letter, we report observation of in-plane AHE in Dirac semimetal Cd_3As_2 films. We have performed measurements on the (112) plane of Cd_3As_2 with the tetragonal D_{4h} structure [32], which possibly allows the onefold and threefold components of in-plane AHE. Figures 1(d)–1(f) show the field-induced Hall conductivity on the (112) plane calculated using an effective model of Cd_3As_2 constructed from previous first-principles calculations [33–36] (see Supplemental Material [37] for details). Notably, a field applied along the in-plane direction $[11\bar{4}]$ or $[\bar{2}12]$ is expected to induce AHE with an amplitude comparable to that induced by the out-of-plane field $B\|[112]$. The threefold component of in-plane AHE corresponds to the average of the three cases with the in-plane field rotated by 120° between each other [dashed line in Fig. 1(f)], which is about one order of magnitude smaller but still remains finite. Through measurements on low-electron-density Cd_3As_2 films, we have succeeded in identifying in-plane AHE appearing with a threefold component following the crystal symmetry. Reflecting its intrinsic origin, in-plane AHE is more pronounced with larger Hall angles in samples with electron density below 10^{17} cm^{-3}. Our demonstration of in-plane AHE broadens the research of Hall physics in nonmagnetic systems, potentially leading to new frontiers focusing on in-plane field-induced orbital magnetization.

(112) Cd_3As_2 films were grown on (111)A CdTe substrate by molecular beam epitaxy [37]. Figure 2 summarizes structural and transport properties of the Cd_3As_2 films. For the epitaxial stacking of (112) Cd_3As_2 on (111)A CdTe, there are three equivalent configurations with either Cd_3As_2 $[11\bar{4}]$, $[\bar{2}12]$, or $[1\bar{2}2]$ parallel to CdTe $[11\bar{2}]$ [Fig. 2(a)]. While it is difficult to identify such 120°-rotated domains by standard x-ray diffraction (XRD) due to the nearly identical lengths of the c axis and the doubled a and b axes, their presence has been reported in the previous

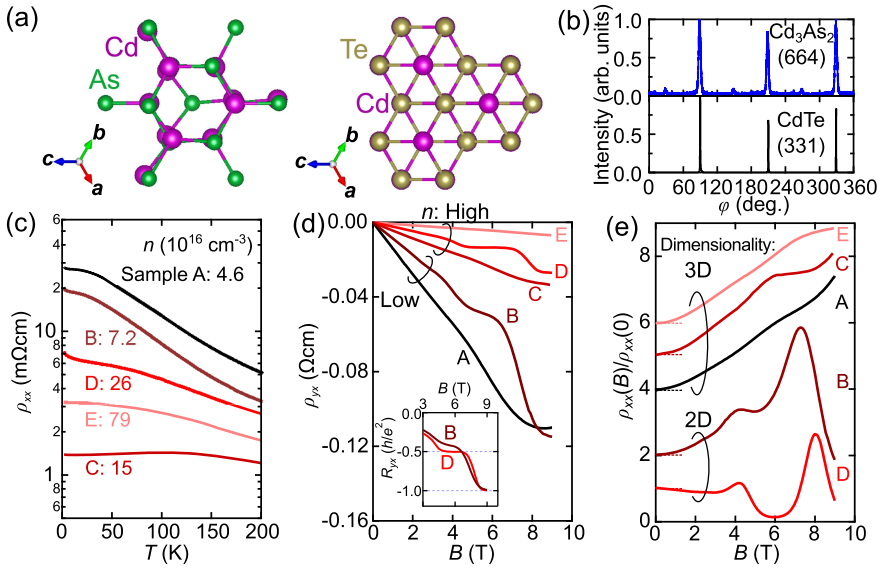

FIG. 2. Structural and transport characterization of Cd_3As_2 films. (a) Top view of the Cd_3As_2 (112) plane and the CdTe (111)A plane. (b) φ scan results of the Cd_3As_2 (664) and CdTe (331) Bragg peaks. The threefold pattern indicates the suppression of the formation of 60°-rotated twins. (c) Temperature dependence of longitudinal resistivity ρ_{xx} of Cd_3As_2 films with different electron density. Out-of-plane field dependence of (d) Hall resistivity ρ_{yx} and (e) magnetoresistivity ratio $\rho_{xx}(B)/\rho_{xx}(0)$. Data are shifted for clarity in (e).

study using the convergent beam electron diffraction technique [42]. Throughout this Letter, we do not distinguish these three in-plane domains since they do mutually attenuate the onefold component of in-plane AHE but contribute equally to the threefold one. As presented in Fig. 2(b), the XRD φ scan of Cd_3As_2 (664) [or (62$\underline{1}$2), (26$\underline{1}$2)] Bragg peak shows that the formation of 60°-rotated twins is highly suppressed in the present Cd_3As_2 films. This is crucial for observing the threefold component of in-plane AHE.

Figure 2(c) presents temperature dependence of resistivity ρ_{xx} for the Cd_3As_2 films with different thicknesses and electron densities [37]. Each sample exhibits a different electron density ranging from 4.6×10^{16} to 7.9×10^{17} cm^{-3}. These low-electron-density Cd_3As_2 films typically exhibit a semiconducting temperature dependence of ρ_{xx}, consistent with the previous report [40]. Figures 2(d) and 2(e) present Hall resistivity ρ_{yx} and magnetoresistivity ratio $\rho_{xx}(B)/\rho_{xx}(0)$ data measured under the out-of-plane field. While thicker films (samples A, C, and E) show positive magnetoresistance accompanied by quantum oscillations, thinner films (samples B and D) exhibit clear development of confinement-induced quantum Hall states [41] with the filling factor $\nu = 1$ or 2 at the high fields. As discussed later, the observed amplitude of in-plane AHE is sensitive to the electron density while the confinement-induced dimensionality change has only a negligible effect.

Next, we present the Hall responses measured under the in-plane field for samples A and B. The azimuthal angle φ of the in-plane field is measured from the CdTe $[11\bar{2}]$ direction, which corresponds to either of Cd_3As_2 $[11\bar{4}]$, $[\bar{2}12]$, or $[1\bar{2}2]$ direction depending on the crystal domain. First, we discuss the results of sample A measured by applying the current along the $\varphi = 270°$ direction as illustrated in Fig. 3(a). Generally, ρ_{yx} measured under the in-plane field involves a magnetoresistance effect, namely, planar Hall effect in its field-symmetric part $\rho_{yx,\mathrm{sym}} = [\rho_{yx}(B) + \rho_{yx}(-B)]/2 = [\rho_{yx}(\varphi) + \rho_{yx}(\varphi + 180°)]/2$, and OHE and AHE in its field-asymmetric part $\rho_{yx,\mathrm{asym}} = [\rho_{yx}(B) - \rho_{yx}(-B)]/2 = [\rho_{yx}(\varphi) - \rho_{yx}(\varphi + 180°)]/2$. To further extract the threefold component $\rho_{yx,\mathrm{AHE}}$, we have subtracted the onefold component from $\rho_{yx,\mathrm{asym}}$, which is mainly derived from the misalignment-induced out-of-plane OHE [37].

As clearly seen in Fig. 3(b), the threefold component emerges as the leading term of in-plane AHE. We note that the threefold φ dependence can be captured even before subtracting the onefold component [37]. The $\rho_{yx,\mathrm{AHE}}$ curves measured at high fields exhibit positive and negative extrema at $\varphi = 0°$ and 60° and their equivalent directions. Since we focus on the threefold component, the observed φ dependence can be understood based on symmetry considerations of the high-temperature Cd_3As_2 phase with the cubic antifluorite structure (point group $Fm\bar{3}m$) [43]. Consistent with the symmetry requirements [13,14], in-plane AHE is prohibited when the field is applied to the $[01\bar{1}]_c$ ($\varphi = 30°$) or its equivalent directions. In each of these directions, there are a C_2 rotational symmetry axis along it and a mirror symmetry plane perpendicular to it.

In order to confirm the reproducibility, we have measured sample B with applying the current to a different direction ($\varphi = 0°$) rotated by 90° as compared to the case of

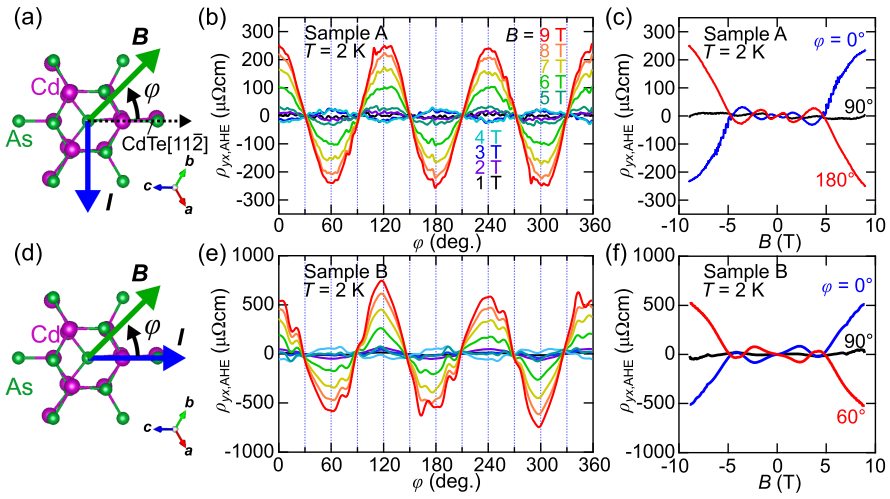

FIG. 3. In-plane anomalous Hall effect observed in Cd_3As_2 films. The azimuthal angle of the in-plane field φ is measured from the CdTe [11$\bar{2}$] direction. (a) Measurement configuration for sample A with the current applied along the direction of $\varphi = 270°$. (b) φ dependence of in-plane anomalous Hall resistivity $\rho_{yx,\mathrm{AHE}}$ measured at different fields, and (c) field dependence of $\rho_{yx,\mathrm{AHE}}$ at different φ for sample A. (d) Measurement configuration for sample B with the current applied along the direction of $\varphi = 0°$. (e) φ dependence and (f) field dependence of $\rho_{yx,\mathrm{AHE}}$ for sample B. In (a) and (d), only one of the three 120°-rotated crystal domains of Cd_3As_2 is illustrated.

sample A, as shown in Fig. 3(d). The $\rho_{yx,\mathrm{AHE}}$ curves obtained for sample B in Fig. 3(e) exhibit the same φ dependence as found for sample A. This highlights the key feature of in-plane AHE being strictly constrained by the crystal symmetry, and hence can be easily distinguished from other onefold effects.

Magnetic field dependence of $\rho_{yx,\mathrm{AHE}}$ is also obtained by subtracting the onefold component from the $\rho_{yx,\mathrm{asym}}$ curve with referring to the φ scans [37]. As presented in Figs. 3(c) and 3(f), $\rho_{yx,\mathrm{AHE}}$ of both samples A and B exhibits a similar unique field dependence, which is composed of an oscillatory behavior below about 5 T and a large enhancement above. This field dependence can be also confirmed in the φ scans in Figs. 3(b) and 3(e).

Since the threefold component effectively emerges as an average of field-induced higher-order effects in the 120°-rotated domains, its field dependence could be nonmonotonic depending on details of the field-induced band modulation and the Fermi level position (see Supplemental Material [37] for detailed discussion). Our model calculation of the threefold component in Fig. 1(f) also shows nonmonotonic field dependence with a sign change, while only a monotonic behavior is expected for each domain. This nonmonotonic in-plane field dependence seems not simply related to the Landau level splitting, considering that it appears in samples A and B regardless of the dimensionality of the electronic structure. Thus, its detailed interpretation remains for future studies.

Figure 4(a) presents temperature dependence of $\rho_{yx,\mathrm{AHE}}$ curves for sample A. The amplitude decays monotonically with increasing temperature, indicating that the field-induced Berry curvature effect is suppressed by increased

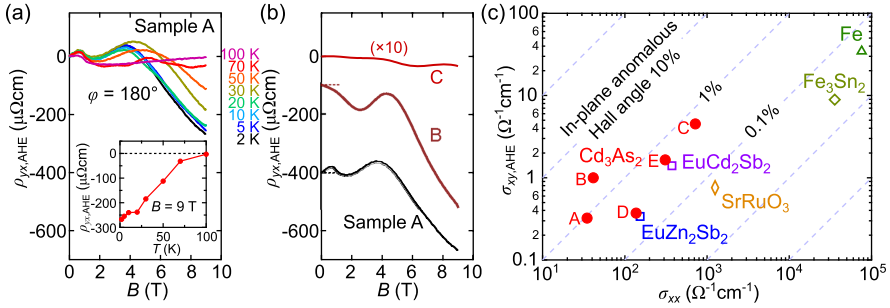

FIG. 4. Temperature and carrier density dependence of in-plane AHE in the Cd_3As_2 films. (a) Temperature dependence of $\rho_{yx,\mathrm{AHE}}$ measured at $\varphi = 180°$ for sample A. Inset shows the change of the $\rho_{yx,\mathrm{AHE}}$ value at 9 T which exhibits a monotonic decay with increasing temperature. (b) Comparison of the field dependence of $\rho_{yx,\mathrm{AHE}}$ to the higher-electron-density film (sample C). Data are shifted for clarity. (c) Relation between the in-plane anomalous Hall conductivity $\sigma_{xy,\mathrm{AHE}}$ and longitudinal conductivity σ_{xx} for the Cd_3As_2 films, compared to other magnetic systems exhibiting in-plane AHE with threefold symmetry: $EuCd_2Sb_2$ [24], $EuZn_2Sb_2$ [25], Fe_3Sn_2 [23], Fe [26], and $SrRuO_3$ [27].

scattering and thermal broadening of the bands at higher temperatures. Figure 4(b) compares the $\rho_{yx,\mathrm{AHE}}$ curves taken for Cd_3As_2 films with different electron densities at $\varphi = 180°$ or its equivalent directions. As represented by sample C, films with electron density higher than 1×10^{17} cm^{-3} exhibit only a small amplitude originating from in-plane AHE (see also Supplemental Material [37]). The in-plane anomalous Hall angle estimated from $\sigma_{xy,\mathrm{AHE}}/\sigma_{xx}$ also exhibits the overall trend that it is more enhanced upon decreasing the electron density [37]. This highlights the intrinsic origin of the observed in-plane AHE. Namely, it is expected to be enhanced as the Fermi level approaches the band degenerate points or band bottoms which become Berry curvature hot spots under the magnetic field.

Figure 4(c) shows the scaling relation between the anomalous Hall conductivity $\sigma_{xy,\mathrm{AHE}}$ and the longitudinal conductivity σ_{xx} obtained for the Cd_3As_2 films. The in-plane anomalous Hall angle of the ultralow-electron-density films (samples A and B) is even larger as compared to previously reported magnetic materials [23–27], and it reaches 2.4% at 2 K. Note that the in-plane AHE of Cd_3As_2 quantified here is only the threefold component. If a single crystalline sample without 120°-rotated domains could be prepared, even larger in-plane AHE with a onefold component can be expected as calculated in Fig. 1(f). Our findings provide a new route for exploring the intrinsic Hall response even in nonmagnetic systems. Quantification of in-plane AHE largely dependent on the carrier density also potentially leads to the demonstration of its quantization as theoretically proposed in previous studies [15–18,22].

In summary, we have extracted large AHE in Dirac semimetal Cd_3As_2 films through systematic measurements under the in-plane magnetic fields. The emergence of the in-plane AHE strictly follows the crystal symmetry of the Cd_3As_2 (112) plane, regardless of the current direction. The obtained in-plane anomalous Hall angle exceeds that of magnetic systems reported previously, suggesting the importance of tuning the Fermi level to achieve large field-induced Berry curvature. The in-plane AHE in nonmagnetic systems can be interpreted as the effect of field-induced orbital magnetization. Together with recent research advances concerning the nonlinear Hall effect [8,9], this Letter demonstrates that the utilization of orbital magnetization leads to exploration of novel physics and functionalities even in nonmagnetic systems.

Acknowledgments—This work was supported by JST FOREST Program Grant No. JPMJFR202N and PRESTO Program Grant No. JPMJPR2452, by JSPS KAKENHI Grants No. JP22K18967, No. JP22K20353, No. JP23K13666, No. JP23K03275, No. JP24H01614, No. JP24H01654, No. JP25H00841, and No. JP25K17947 from MEXT, Japan, by Toyota Riken Rising Fellow Program funded by Toyota Physical and Chemical Research Institute, Japan, by Murata Science and Education Foundation, Japan, by STAR Award funded by the Tokyo Tech Fund, Japan, and by Iketani Science and Technology Foundation, Japan.

Data availability—The data that support the findings of this Letter are available from the corresponding author upon reasonable request.

[1] N. Nagaosa, J. Sinova, S. Onoda, A. H. MacDonald, and N. P. Ong, Rev. Mod. Phys. **82**, 1539 (2010).
[2] L. Šmejkal, A. H. MacDonald, J. Sinova, S. Nakatsuji, and T. Jungwirth, Nat. Rev. Mater. **7**, 482 (2022).
[3] D. Xiao, M.-C. Chang, and Q. Niu, Rev. Mod. Phys. **82**, 1959 (2010).
[4] J. H. Cullen, P. Bhalla, E. Marcellina, A. R. Hamilton, and D. Culcer, Phys. Rev. Lett. **126**, 256601 (2021).
[5] H. Wang, Y.-X. Huang, H. Liu, X. Feng, J. Zhu, W. Wu, C. Xiao, and S. A. Yang, Phys. Rev. Lett. **132**, 056301 (2024).
[6] P. Streda, J. Phys. C **15**, L717 (1982).
[7] N. Ito and K. Nomura, J. Phys. Soc. Jpn. **86**, 063703 (2017).
[8] J. Son, K.-H. Kim, Y. H. Ahn, H.-W. Lee, and J. Lee, Phys. Rev. Lett. **123**, 036806 (2019).
[9] K. Kang, T. Li, E. Sohn, J. Shan, and K. F. Mak, Nat. Mater. **18**, 324 (2019).
[10] T. Liang, J. Lin, Q. Gibson, T. Gao, M. Hirschberger, M. Liu, R. J. Cava, and N. P. Ong, Phys. Rev. Lett. **118**, 136601 (2017).
[11] T. Liang, J. Lin, Q. Gibson, S. Kushwaha, M. Liu, W. Wang, H. Xiong, J. A. Sobota, M. Hashimoto, P. S. Kirchmann, Z.-X. Shen, R. J. Cava, and N. P. Ong, Nat. Phys. **14**, 451 (2018).
[12] Y. Liu, H. Wang, H. Fu, J. Ge, Y. Li, C. Xi, J. Zhang, J. Yan, D. Mandrus, B. Yan, and J. Wang, Phys. Rev. B **103**, L201110 (2021).
[13] T. Kurumaji, Phys. Rev. Res. **5**, 023138 (2023).
[14] J. Cao, W. Jiang, X.-P. Li, D. Tu, J. Zhou, J. Zhou, and Y. Yao, Phys. Rev. Lett. **130**, 166702 (2023).
[15] X. Liu, H.-C. Hsu, and C.-X. Liu, Phys. Rev. Lett. **111**, 086802 (2013).
[16] Y. Ren, J. Zeng, X. Deng, F. Yang, H. Pan, and Z. Qiao, Phys. Rev. B **94**, 085411 (2016).
[17] J. Zhang, Z. Liu, and J. Wang, Phys. Rev. B **100**, 165117 (2019).
[18] S. Sun, H. Weng, and X. Dai, Phys. Rev. B **106**, L241105 (2022).
[19] L. Li, J. Cao, C. Cui, Z.-M. Yu, and Y. Yao, Phys. Rev. B **108**, 085120 (2023).
[20] Y. D. Wang, Z.-G. Zhu, and G. Su, Phys. Rev. Res. **5**, 043156 (2023).
[21] L. Xiang and J. Wang, Phys. Rev. B **109**, 075419 (2024).
[22] W. Miao, B. Guo, S. Stemmer, and X. Dai, Phys. Rev. B **109**, 155408 (2024).
[23] L. Wang, J. Zhu, H. Chen, H. Wang, J. Liu, Y.-X. Huang, B. Jiang, J. Zhao, H. Shi, G. Tian, H. Wang, Y. Yao, D.Yu, Z. Wang, C. Xiao, S. A. Yang, and X. Wu, Phys. Rev. Lett. **132**, 106601 (2024).

[24] A. Nakamura, S. Nishihaya, H. Ishizuka, M. Kriener, Y. Watanabe, and M. Uchida, Phys. Rev. Lett. **133**, 236602 (2024).
[25] H. Lee, S. Nishihaya, M. Kriener, J. Fujioka, A. Nakamura, Y. Watanabe, H. Ishizuka, and M. Uchida, Phys. Rev. B **111**, L241106 (2025).
[26] W. Peng, Z. Liu, H. Pan, P. Wang, Y. Chen, J. Zhang, X. Yu, J. Shen, M. Yang, Q. Niu, Y. Gao, and D. Hou, arXiv:2402.15741.
[27] S. Nishihaya, Y. Matsuki, H. Kaminakamura, Y. Murakami, H. Ishizuka, and M. Uchida, arXiv:2502.10018.
[28] J. Zhou *et al.*, Nature (London) **609**, 46 (2022).
[29] E. Lesne, Y. G. Sağlam, R. Battilomo, M. T. Mercaldo, T. C. v. Thiel, U. Filippozzi, C. Noce, M. Cuoco, G. A. Steele, C. Ortix, and A. D. Caviglia, Nat. Mater. **22**, 576 (2023).
[30] Y. Cui, Z. Li, H. Chen, Y. Chen, Y. Wu, K. Pei, T. Wu, N. Xie, R. Che, X. Qiu, Y. Liu, Z. Yuan, and Y. Wu, Sci. Bull. **69**, 2362 (2024).
[31] M. Wang, J. Zhang, D. Tian, P. Yu, and F. Kagawa, Commun. Phys. **8**, 28 (2025).
[32] M. N. Ali, Q. Gibson, S. Jeon, B. B. Zhou, A. Yazdani, and R. J. Cava, Inorg. Chem. **53**, 4062 (2014).
[33] Z. Wang, H. Weng, Q. Wu, X. Dai, and Z. Fang, Phys. Rev. B **88**, 125427 (2013).
[34] P. V. Arribi, J.-X. Zhu, T. Schumann, S. Stemmer, A. A. Burkov, and O. Heinonen, Phys. Rev. B **102**, 155141 (2020).
[35] S. Baidya and D. Vanderbilt, Phys. Rev. B **102**, 165115 (2020).
[36] M. Smith, Victor L. Quito, A. A. Burkov, P. P. Orth, and I. Martin, Phys. Rev. B **109**, 155136 (2024).
[37] See Supplemental Material at http://link.aps.org/supplemental/10.1103/5d7l-mr7k for details of film growth, fundamental properties of studied samples, model calculation of the in-plane anomalous Hall conductivity, procedures for extracting the in-plane anomalous Hall component, and electron density dependence. The Supplemental Material also contains Refs. [24,30,31,33–36,38–41].
[38] T. Liang, Q. Gibson, M. N. Ali, M. Liu, R. J. Cava, and N. P. Ong, Nat. Mater. **14**, 280 (2015).
[39] A. Narayanan, M. D. Watson, S. F. Blake, N. Bruyant, L. Drigo, Y. L. Chen, D. Prabhakaran, B. Yan, C. Felser, T. Kong, P. C. Canfield, and A. I. Coldea, Phys. Rev. Lett. **114**, 117201 (2015).
[40] Y. Nakazawa, M. Uchida, S. Nishihaya, S. Sato, A. Nakao, J. Matsuno, and M. Kawasaki, APL Mater. **7**, 071109 (2019).
[41] M. Uchida, Y. Nakazawa, S. Nishihaya, K. Akiba, M. Kriener, Y. Kozuka, A. Miyake, Y. Taguchi, M. Tokunaga, N. Nagaosa, Y. Tokura, and M. Kawasaki, Nat. Commun. **8**, 2274 (2017).
[42] H. Kim, M. Goya, S. Salmani-Rezaie, T. Schumann, T. N. Pardue, J.-M. Zuo, and S. Stemmer, Phys. Rev. Mater. **3**, 084202 (2019).
[43] A. Pietraszko and K. Lukaszewicz, Acta Crystallogr. Sect. B **25**, 988 (1982).